University of New Mexico

Mesh Adaptation Based on the Depth Image (MABDI)

A thesis proposal submitted in partial fulfilment for the degree of Masters of Science

Lucas Chavez
lucasc@unm.edu

Department of Mechanical Engineering
University of New Mexico

Advisor
Dr. Ron Lumia

March 2013

Contents

1 Goal

The goal of this work is to design a method which can create a reliable mesh representation of the environment from sequential registered noisy point cloud data sets. We will name this method MABDI which stands for Mesh Adaptation Based on the Depth Image. The method must be computationally feasible for online applications and have a low memory requirement. In addition, the method must update the representation when new measurements of revisited parts of the environment are made.

2 Problem

A rich representation of an environment is essential for most autonomous systems because it allows the agent or operator to have an increased situational awareness of the world. The methodology to build this representation is a continuously evolving subject in the field of robotics. The origins of the research into this problem date back roughly 25 years. Since then the methods and the representations themselves have continued to evolve at an impressive rate. The main catalyst behind this growth is the advancement of sensing technologies over the same time period. In general, sensors have continued to generate measurements at higher rates, higher resolution, and lower cost over the years. This has provided an amazing opportunity to build richer and more useful representations of the environment.

In robotics map building in an unknown environment is referred to as the Simultaneous Localization and Mapping (SLAM) problem. This label describes the fact that a methodology which solves the SLAM problem must simultaneously locate the robot in the environment as well as map the environment. The methodology by which the representation is built is called mapping and is the focus of this work. Early mapping methods represented the environment as a set of landmark locations. The result was a sparse set of points usually on a 2D plane. This allowed research to show that their SLAM solutions worked but it soon became clear that a richer representation of the world was needed for a growing number of applications. In response several methods were developed using various other representations. A number of representations are compared in Table 1.

Table 1 compares the characteristics of map the representations. Adaptability describes the ability of the representation to correct itself given new information. Computational expense describes how difficult it is to create and maintain a representation. Memory requirement describes how much memory a method must use to run. Situation Awareness (SA) describes how well suited a representation is for both robot and human decision making. Robot decision making requires a representation that can be used for such problems as obstacle avoidance. Human decision making requires a method that can be allow an operator to intuitively understand the state of the robot given

Table 1: Characteristics of current forms of representation

	Adaptability	Computationally Inexpensive	Low Memory Requirement	SA: Robot	SA: Human
Landmark Locations	x	x	x	-	-
Point Clouds	-	x	-	-	-
Surfels	x	x	x	-	x
Implicit Functions	x	-	-	x	x
Static Mesh	-	x	x	x	x
Adaptive Mesh	x	o	o	x	x

the map. The Table is supposed to reflect what a representation is capable of and not necessarily where the state-of-the-art is.

A mesh based representation is arguably an extremely good choice in comparison to the other representations. It has been used extensively by the gaming community because it is the best for representing large environments with the minimum memory. Also, this sort of representation works well to increase the SA of a robot because methods for performing physical simulations such as obstacle collision detection already exist. In addition, a mesh based environment is a very natural method to display information to a human operator.

Currently, the problem with mesh-based environmental mapping techniques is that they are greedy in the sense that the mesh elements can not be corrected using new information. Once the mesh is in place there is no mechanism to adapt to newer measurements. The problem of adapting a mesh to new information is a very well studied problem in computer graphics, but these methods were not designed with large scale environmental mapping in mind. The biggest questions are:

- How can we quickly decide which measurements should be used to adapt which part of the mesh?
- How can we quickly detect new and removed objects?
- How can we robustly deal with noise and obtain a methodology that makes use of the new measurements of an already existing part of the representation?

So the real question is can we develop a methodology that can address all of the above questions and still have a manageable memory requirement and be computationally feasible? The goal of this work is to show that MABDI is capable of addressing these questions.

3 State of the Art

A major problem in robotics has been and continues to be: How can we create the "best" representation of an unknown environment? There are two main communities of researchers who been working on developing algorithms and methods to answer precisely this question. They are the robotics community and the computer graphics community and each community has a slightly different motivation for solving this problem. The robotics community is concerned with developing a real-time solution of generating representations in large environments. These representations are used by both fully autonomous and teleoperated systems. The common name which is used by the robotics community for this problem is Simultaneous Localization and Mapping or SLAM. The name SLAM refers to the problem of mapping and locating a robot in an unknown environment. Early methods generated very sparse representations of the world, as time and sensor technology progressed the representations became denser. A dense representation is desired for any system which must have good situational awareness of its environment. The computer graphics community is concerned with generating high quality representations of smaller environments and single objects. They generally refer to the problem as surface reconstruction. These representations are used by augmented reality, computer game object creation, 3D printing, and more applications. In the following sections we will trace the development of representation generating methods in both communities. We will then discuss what is needed in future work.

3.1 SLAM

The problem of SLAM has been a primary focus of the robotics community for more than 25 years. A complete solution to the SLAM problem must be able to generate a representation of an unknown environment and track the robot in this new representation. In this body of literature the act of generating a representation is referred to as mapping. A good overview of the problem can be found in [1] and [2]. Each solution is designed to consider the goal application, type of sensor, computational constraints, and memory limits. All these factors influence the researcher's choice of what type of representation to use for the mapping procedure. In 2002 Thrun wrote a famous survey [3] of the SLAM literature which categorized existing algorithms on many traits including the representation. The representation choice of prior work can be roughly categorized into 3 types. The first type is characterized by some sort of list of 2D or 3D points and are usually considered to be sparse representations. Common names for these types are landmark locations and point clouds. The second type are considered to be more volumetric based and are often times considered to be a dense representation. Common names for these types are occupancy grid and Truncated Signed Distance Function (TSDF). The last type have the characteristic of being a surface representation and are also considered to be a dense representation. Common names for these types are surfels and mesh. In the following sections we will trace the history of each of the

3 types of representation that is seen in the SLAM literature.

3.1.1 Point Locations

One of the most well known and earliest solution to the SLAM problem, which uses a point location representation, was proposed by Smith et al. in 1990 [4]. The mathematical framework that he created was the origin of a family of solutions based on the Extended Kalman Filter (EKF). The representation he chose was simply a list of 2D landmark locations. Each location was part of a state matrix which was estimated at every iteration. A list of landmark locations was chosen because it allowed the method to have a low computational cost and use a small amount of memory, important factors in the days of early computing. There have been many improvements to the family of SLAM solutions which generate a list of point locations since Smith's work. One of the first practical implementations on a real robot was done by Thrun in 1998 [5]. In this work the SLAM problem was posed in an Expectation Maximization (EM) framework which is similar to the EKF framework in that landmark locations are saved in a state vector which is estimated at every iteration. In Thrun's work an occupancy grid map is generated as a post processing step from sonar measurements. The results showed that their representation could become more accurate over time by using new observations to improve the current estimate. This a highly desired ability of any representation generation method. The next step was the ability of these methods to include a loop closure procedure. A loop closure procedure was proposed by Gutmann in 1999 [6]. The key ability of the method was it could recognize when the robot was revisiting a prior location and adjust the entire representation with the constraint that the two points must coincide. In 2001 Dissanayake et al. [7] derived 3 theorems to theoretically prove the convergence of the SLAM problem. Their test platform used a millimeter-wave radar mounted on a vehicle and generated a list of 2D landmark locations. In 2001 Thrun et al. [8] cast the SLAM problem using particle filter techniques. Their results generated a 2D map and showed an increased robustness and lower computational cost than prior methods. One of the key disadvantages of methods up to this point was that complexity scaled quadratically with the number of landmark locations. In 2002 Montemerlo et al. [9] created a SLAM solution named FastSLAM which was able to handle a much larger number of landmarks. They showed results with maps containing more than 50,000 points. Then, SLAM solutions using point locations became much more directed towards 3D.

Some of the first interesting works which represented the world as a list of 3D point locations were done by Thrun et al. in 2000 [10], Liu and Emery in 2001 [11], and Hähnel et al. in 2003. In these works the 2D landmark locations and robot position were estimated using very similar techniques from past work. Once this had been done the 3D laser scan data was simply appended to each estimated robot location. Then, a mesh was created by post processing the 3D point cloud. They utilized the fact that the laser collected the data in an incremental manner and simply connected neighboring 3D points. Finally, the mesh was simplified by looking for large planar

sections and merging the corresponding mesh elements. One of the first SLAM solutions which used a single camera to generate a list of 3D points was done by Davison in 2003 [12]. Here he used a single camera to generate a very sparse list of 3D points. This method was limited to small environments. Future advances allowed representations of larger environments. In 2003 Thrun et al. [13] created a SLAM procedure which did not rely on having a structured environment and was applied to mapping large mines. In 2004 Howard et al. [14] created a SLAM systems based on a Segway platform equipped with a 3D laser which could map large areas of roughly 0.5 km on each side. One of the results showed a map with approximately 8 million points. In 2006 Cole and Newman [15] continued work in large-scale SLAM by increasing robustness and also generated maps with many 3D points using a laser sensor. In 2007 Clemente et al. created a large-scale SLAM system that used a single camera. The system had an advanced loop closing procedure based on visual features and created large maps of 3D points. In 2001 Klein and Murray [16] developed a SLAM solution which used a single camera. The uniqueness of their method was the algorithmic structure. Their SLAM solution consisted of 2 separate processes: a tracking processes and a map building process. This algorithmic structure has become very common in many current SLAM solutions because of the advances in pose estimation technology. Klein and Murray were able to get very good results for a small environment and showed Augmented Reality (AR) applications. Many of the future advances of SLAM solutions, which generated 3D point sets, dealt with camera systems [17, 18, 19] and improved in speed and robustness. Many of the most current methods which produce a list of points are systems that use a relatively new type of sensor named a RGB-D sensor. One good example is a work that was produced in 2011 by Engelhard et al. [20]. In this work they used an algorithm named the Iterative Closest Point (ICP) [21] to align point clouds from coming from the RGB-D sensor into a large colored point cloud. The resulting maps were visually impressive. However, the map could not be adapted to new information and was not well suited for other applications, such as obstacle avoidance. These limitations are inherent in maps that consist of lists of points.

3.1.2 Volumetric

Many SLAM solutions generate a 2D volumetric representation of the world because they are especially advantageous in dealing with noisy sensors. Two of the first major works which generated a 2D volumetric representation were done in 1998 by Yamauchi et al. [22] and Schultz et al. [23]. These works generated a 2D occupancy grid which is a type of volumetric representation. Here the environment was divided into a 2D grid. Each square of the grid contained the probability that it was occupied with an object. All squares would be updated iteratively based on the current sensor readings. Occupancy grids, like any other volumetric-based representation, are limited by the amount of available memory. In 2002 Biswas et al. [24] extended occupancy grid methods by allowing dynamic environments. This was done by looking at past "snapshots" of the map.

In 2004 Eliazar and Parr [25] continued the advancement by decreasing computational cost and implemented a loop closure method.

There have been a few impressive SLAM solutions which generate a 3D volumetric representation. There are three major works which generated something very similar to a 3D occupancy grid which was saved as in a octree data structure [26, 27, 28, 29]. Each work had a slightly different name and procedure for generating the representation, but in general the representations divided the environment into cubes and had a scalar value representing the belief of a surface being there. Octrees were used to save memory by only having a fine resolution of cubes at places where there was a surface. There are many advantages to a 3D occupancy grid representation. When applied to obstacle avoidance and path planning algorithms. Also, the representation is very adaptable to new information. The major disadvantage is that the representation can not be visualized immediately. In order to render, an image must be generated at each desired viewpoint by ray tracing the volume. This can be a problem when using such method for applications such as teleoperation due to the computational cost of rendering. The current state of the art for generating a volumetric representation was done by Newcombe et al. in 2011 [30]. Their system used a RGB-D sensor and generated a 3D voxelized grid Truncated Signed Distance Function (TSDF) of the environment. For this type of representation each cube contains the value of the distance to the nearest surface. The sign of the value is based on which side of the surface the cube is relative to the sensor. This work has been the most capable at dealing with extremely noisy data and dynamic scenes. However, due to memory constraints the method can only represent environments that are about the size of a 4m cube. Also, it must be ray traced in order to be visualized.

3.1.3 Surface

One of the first major works which created a surface representation of the environment in real-time was done by Martin and Thrun in 2002 [31]. Their method utilized an EM framework to fit plane models to 3D point cloud data. Polygon mesh elements were then easily assigned to each plane. The main drive behind this work was to generate a map of the environment that uses a low amount of memory. Their method worked well for structured environments. One of the major limitations of their method, and other methods that only mesh large planar sections, is that the representation will only consist of planar sections and not capture the fine detail of the environment. In 2004 Viejo and Cazorla [32] developed a methodology for generating a mesh that can contain more information of the environment than large planar sections. Due to this ability, they termed their method to be "unconstrained." Essentially their method was based on a 3D Delaunay triangulation algorithm. Giesen surveyed Delaunay triangulation methods in [33]. Viejo and Cazorla were not able to obtain real-time results and, in fact, it has been seen that it is extremely difficult to run a 3D Delaunay triangulation in real time because of the numerous amount of distance calculations that are needed. One of the next major advances came from Weingarten and Siegwart in 2006 [34]. Their work also

created a mesh that was only capable of capturing large planar surfaces. However, they showed increased robustness. In 2007 Pollefeys et al. published a work with multiple researchers [35, 36]. They developed a large urban mapping system consisting of a vehicle and eight camera systems. The processing was carried out by multiple CPUs and optimized with Graphics Processing Unit (GPU) calculations. In their work they used the camera systems to generate depth maps. The set of depth maps was then fused to create a new smaller set of depth maps that were more accurate. The depth maps in the smaller set were more accurate because the error was averaged out by using near-by depth maps. The smaller set was then used by a triangulation procedure to create a mesh of the environment. The mesh generation procedure was based on a work from 2002 by Pajarola et al. [37]. This method defines a mesh in the depth image. It starts from a very coarse mesh and continues to refine in areas of the depth image based on a confidence criteria. In the work of Weingarten and Siegwart these meshes which are defined for each fused depth image are then checked for overlaps and duplicates are removed to make a single large mesh. One of the major drawbacks of this approach is that the output mesh can not be adapted by measurements which come from revisited parts of the scene. Another major advancement came in 2008 from Poppinga et al. [38]. In this work they used a Time of Flight (ToF) camera to generate a mesh representation of the large planar structures in the environment. Here they also develop a procedure to determine a mesh in a depth image. They leverage the structure of the depth image to make the method computationally inexpensive. In their work they simply append the meshes which are created from each depth image into a global coordinate system. They obtain very good results from a simple method. Once again, the method is not adaptive to new information. Also, a mesh is created for each depth image instead of updating and maintaining a global mesh. A major advancement came from a famous work done by Newcombe and Davison in 2010 [39]. In this work they designed a method to create a mesh reconstruction from a single video camera. Their method used Structure From Motion (SFM) to obtain a sparse point cloud of the scene. Then an implicit function was fit to the point cloud using the methodology of Ohtake et al. [40]. A bundle of depth maps is then selected. From the bundle a single reference depth image is selected and a "base" model is constructed by sampling the implicit surface for vertices in the reference frame. The neighboring frames are used to better the "base" model and create a more accurate mesh. Each reference frame has its own mesh and all the meshes are put into a global coordinate system. Duplications are then detected and removed. Again, the representation is not adaptive to new information. In 2010 Stühmer et al. [41] advanced the field by publishing a method to generate very accurate depth maps from several color images in real-time. They showed very impressive results but their method was not designed to maintain a representation in a global coordinate frame.

The next major advances in methods that generated surface representations of the environment, were based on RGB-D sensors.This type of sensor has become very popular since the release of the Kinect from Microsoft which was the first mass produced RGB-D sensor of its kind. RGB-D sensors are inexpensive and produce noisy 640x480 depth images at 30Hz. The RGB-D sensor

has excited the robotics community because this has been the first time that depth data has been so readily accessible from such an inexpensive sensor. Therefore, these methodologies must be able to quickly deal with very high rates of information. One very impressive work came from Henry et al. in 2012 [42]. In this work they designed a system which used a RGB-D sensor to build a map made of surfels. In order to generate and maintain the surfel map they used the work of Weise et al. [43]. Surfels are circular disks which have a particular position and orientation and also a radial size based on confidence. The map consists of a large number of surfels. The surfel map can be updated given the new registered depth images from the sensor. Decisions are made of how to handle each measurement in the depth image based on the difference between an expectation generated using the current map and the actual readings from the sensor. Rendering a surfel map requires special methods [44] and is difficult to use in applications such as obstacle avoidance. One of the next major advances was published by Whelan et al. in 2012 [45] and more recently in 2013 [46]. The system they developed was named Kintinuous and was able to produce a high quality mesh representation of the environment. Their system was a hybrid system and utilized the KinectFusion method [30] of Newcombe et al. to create a volumetric representation of the portion of the environment in front of the sensor. As the sensor moves, portions of the environment that leave the volume in front of the sensor are ray cast and turned into a mesh. They obtain very impressive results but also mention a limitation of their system for future work. The limitation is that the mesh can not be updated once created, which is an issue when revisiting parts of the environment. One of the most impressive current works which has an adaptable mesh came from Cashier et al. in 2012 [47]. In this work, they were able to generate and update a mesh with new measurements from a ToF sensor. They used the difference between the existing model and the actual measurements to decide whether to adapt the mesh or add new elements. The mesh topology was not adaptive to the environment and their experiments only showed results of mapping a single flat wall with no robot movement. The system needs to be tested for object addition and removal.

3.2 Surface Reconstruction

The computer graphics field has spent considerable effort to develop methodologies for creating representations from sets of data. Generally, these sets of data are acquired from a sensor. Methodologies have progressed steadily and are often designed for a specific application. One of the original motivations was to generate surfaces from medical imaging data. This allows doctors to make better decisions because the data are presented in a more intuitive manner. Current applications include augmented reality and 3D printing. Older methodologies were not as concerned with speed and often times had a large computational cost. Also, the methodologies are often designed for single objects or small environments. Following the taxonomy of such well-known works as [48, 49], the field can be roughly divided into representations that are generated with volume-based techniques and those that use surface-based techniques. Methods that use volume-based techniques

are characterized by spatially subdividing the environmental volume and are usually computationally expensive and require a large amount of memory. Methods that use surface-based techniques generate the representation using surface properties of the input data. Both types of methods can have mechanisms to adapt the mesh to noisy or new information. In the following section we will trace the progression of the methodologies.

3.2.1 Volume-based

Volume-based methods spatially subdivide the volume into smaller parts and operations are performed on the mesh to either implicitly imply the surface or define the surface depending on the information contained in each subdivision. One of the first well-known works that used a volume-based technique was proposed by Lorensen and Cline in 1987 [50]. In this work they proposed a method named marching cubes which is still known for its reliability and simplicity and is used by applications which do not have a computational requirement. Marching cubes subdivides the space into cubes. The data contained in each cube dictate how the surface connectivity will be defined in that cube. Possible vertex locations are at the corners and along the edges. Once this has been done for all cubes the process is complete. One of the next major steps came from Hoppe et al. in 1992 [51] In this work they used the input points to define a Signed Distance Function (SDF) in 3D space and then meshed the zero-set to obtain the output mesh. A SDF is a spatial function which has the value of the distance to the nearest surface at each point. The sign is used to specify if the point is inside our outside of the surface relative to the sensor. The zero-set of the SDF is the surface where the values transition from positive to negative. Using a SDF has proven to be very effective and has been the core idea of many methodologies that came after this work of Hoppe et al., such as KinectFusion [30]. One of the next advances came from Edelsbrunner and Mücke in 1994 [52] with a method named alpha shapes. Here they used 3D Delaunay triangulation and the input point set to decompose the volume into a Delaunay tetrahedrization. This gives a triangulation of the input set which involves all points. A sphere of radius alpha is then used to remove edges and vertices to obtain a mesh of user specified resolution. Many works have made use of 3D Delaunay triangulation to create a mesh. Methods which use 3D Delaunay on the input set have a large computational cost and often cannot be executed in real-time. The next valuable contribution came from Bloomenthal in 1994 [53] as open source software for surface polygonization of implicit functions. This was a stable and robust open source software that has been used in many well-known algorithms [39]. Another major advance came from Curless and Levoy in 1996 [54]. In this work they also constructed a Truncated Signed Distance Function (TSDF). A TSDF is very similar to a SDF, the only difference is that distance values are truncated after they exceed a certain threshold. Their method was one of the first to be able to handle several registered range scans. Their work showed how well a TSDF can deal with several noisy scans by naturally integrating out the error. They obtained very good results but not even close to real-time. A speed up in processing

time was achieved by Pulli et al. in 1997 [55] by utilizing octrees. They obtained good results and their method was used by Surmann et al. [56] in a well-known robotic mapping work. Another major advance came in 2001 from Zhao et al [57]. They used Partial Differential Equation (PDE) methods to obtain a final reconstruction that was of better quality than prior methods. In 2001 Carr et al. [58] created a volumetric method based on the radial basis function (RBF). Their method was able to successfully deal with holes and generate water tight models. A water tight model is useful for single object reconstruction. However, it is not desired for mapping large environments. One of the next major advances was published in 2003 by Ohtake et al. [40]. In this work they created a method which was faster than the work of Carr et al. [58] by implementing a hierarchical approach with compactly supported basis functions. Their work has been considered to be the state of the art for calculating an implicit function of a noisy point set and was used by Newcombe et al. [39]. Volume-based methods have been able to create high quality representations and work well for single objects and small environments. These methods must spatially divide the environmental volume and therefore have a high memory requirement.

3.2.2 Surface-based

One of the first interesting and adaptive surface-based methods was published by Terzopoulos and Vasilescu in 1991 [59] and dealt with 2.5D data such as intensity and range images. The goal of their work was to create an adaptive mesh of an input image. The mesh was initialized as a 2D sheet of mesh elements with virtual springs along each edge. The stiffnesses of the virtual springs would then adjust based on the image information at that location. The mesh was able to adapt to be more dense in regions of higher intensity. In 1992 Terzopoulos and Vasilescu extended their methodology to 3D data [60]. In this work they used the distance between the mesh and the data to drive the vertices to be near the surface. In this early work they needed to initialize the mesh and control the subdivision of mesh elements to obtain a suitable resolution. In 1993 Hoppe et al. [61] published a method to optimize to resolution of a given mesh by posing the problem in an energy minimization framework. They minimized an energy function which tried to adequately represent the surface in the most concise mesh possible. One of the next advances in physical based adaptation of meshes came in 1993 from Huang and Goldof [62]. In this work they were able to adjust the size of the mesh elements to obtain a better resolution in areas of high frequency information using a physical based model. In addition, it was one of the first works to represent an object undergoing deformation. They method was able to perform tracking on simple simulation examples. Another advancement came in 1994 Rutishauser et al. [63] with a method specifically designed for incremental data. Their methodology worked with a sequential input set of range data and used a probabilistic framework to adjust the vertices of a mesh to the expected value given the prior observations. Their methodology also modeled the noise of the sensor with a sensor model. In 1994 Delingette [64] developed a methodology to generate a simplex mesh model of structured and

unstructured 3D datasets. Elastic behavior of the mesh surface was modeled by local stabilizing functionals. Also, they implemented an iterative refinement process to refine the mesh in areas of high frequency information. One of the next steps was published by Turk and Levoy in 1994 [65]. Their method allowed overlapping meshes to be "zippered" into a single mesh surface. This ability is especially important for methods that generate a mesh for each depth image of the sensor and then need to combine all registered meshes into a single mesh. Their method is computationally expensive due to distance calculations. An interesting work came in 1995 from Chen and Medioni [66]. They devised an adaptive mesh methodology based on the inflation of a balloon. A mesh sphere was first initialized within the registered range measurements of the object. Virtual inflation forces were then used to expand the balloon until the mesh surface was a minimal distance from the range data. This method was limited to objects which are water tight. A major advancement came in 1999 from Bernardini et al., [67] in a method named the ball-pivoting algorithm. Their method is a good example of an advancing front method. These types of algorithms start with a seed mesh element and advance the boundary by adding new mesh elements in the immediate area of the boundary which is supported by measurements. Most advancing front algorithms differ in how it is decided to add new mesh elements. In the work of Bernardini et al. a virtual sphere of a user defined radius is rolled along the boundary of the mesh and new elements are added if the ball touches another measurement. Their methodology became popular because of its simplicity. One major disadvantage was that the generated mesh was a fixed topology. Another advancing front method came in 2001 from Gopi et al. [68, 48]. Here they sampled the input dataset to obtain a new dataset with a lower density of points in areas of lower frequency information. This effectively gave their method an adaptive topology. Next, a local neighborhood was computed at each data point and projected to a plane tangent to the surface. The triangulation is then computed on this local tangent plane. They obtained impressive results on datasets of varying sample density and curvature. An interesting work was published in 2003 by Ivrissimtzis et al. [69]. Here they used a neural network model to adapt a mesh model to the data. They claimed that their method is computationally independent of the size of the input dataset because the dataset is only sampled by the method. There obtained good results. In 2004 Alexa et al. published a very interesting work to generate point set surfaces from an input dataset [70]. They use moving least squares (MLS) to locally approximate the surface with polynomials. The original dataset is then no longer used. Instead, they develop tools to sample the approximated surface to any resolution desired so that the end result is another point set of user specified resolution lying closer to the surface than the input dataset. One drawback is they had to develop their own methodology to render a point set. In 2005 Scheidegger et al. used the work of Alexa et al. to develop an advancing front methodology to generate concise meshes of high accuracy. Their main contribution was to augment an advancing front algorithm with global information so that the triangle size could adapt gracefully to any change. They obtained very impressive results. Most methodologies in Surface Reconstruction had been solely concerned with object or small environment recreation and have

computational or memory requirements which do not work well with large environments. One of the first successful methods intended for large environments was published in 2009 by Marton et al. [71]. Their methodology was an advancing front algorithm which worked on a point set which was sampled from the MLS surface of the original point set. They were able to obtain impressive and near real-time results on datasets of large environments. They also developed a method to deal with revisited parts of the scene by determining the overlapping area and reconstructing only the updated part of the surface mesh. While this is a step forward, it would be better if the mesh surface converged to the actual surface with an increasing number of measurements. To support dynamic scenes they developed mechanisms to decouple and reconstruct the mesh quickly. They only discussed these mechanisms in theory and had no results of how these mechanisms work. While Surface-based Surface Reconstruction techniques have developed impressively, several key issues arise when applying these techniques to mapping large environments.

3.3 Summary

The fields of Robotics and Computer Vision have developed many exciting methodologies to construct representations from a noisy input dataset. However there is still work to be done to obtain the ideal reconstruction method. A mesh is clearly a desirable type of representation and an efficient method should be able to generate and maintain a mesh representation. Also, many existing methods do not leverage the inherent structural information contained within the depth image. There are imaging processing techniques that could be used to answer some of the remaining problems in surface reconstruction, such as the need for adaptive topology and the need to decide how each measurement should be used to update the existing mesh. Henry et al. [42] has already investigated using the difference between the expected and actual measurements to guide the decision of how to use each measurement. However, their work was intended for surfels and needs to be extended to meshes. A method to generate a representation is needed which is computationally and memory efficient and can better adapt the representation to new information.

4 Contribution

MABDI will contribute to the state of the art in two main ways. First, MABDI will leverage the difference between the actual and expected depth image to quickly classify the measurements of the depth image into those that are new, those that support a preexisting surface, and those that are from a new or removed object. The method to perform this categorization has never been performed on a depth image. The advantage of performing it on the depth image is that computationally efficient machine imaging techniques can be used. Once the classification has been performed the appropriate actions can be taken with each measurement. Second, MABDI will generate mesh

elements using the current depth image. Image processing techniques will be used to make the mesh topology adaptive to the frequency content of the scene so that large surfaces, such as walls, will be represented with fewer vertices while complex objects will be represented with more. This will be the first time that the mesh topology will adapt by using image processing techniques to acquire a good guess of the frequency content in the scene.

5 Impact

There are two main areas which will benefit from a methodology for generating a rich mesh based representation of the environment, such as the MABDI method. Both of these areas are driven by the need for good situational awareness of the environment. The first area is robotic decision making. There are many classical robotic applications that seek to reason and make decisions about the environment in which the robot is working. One example is object manipulation with a robotic arm. There are many developed methods which use physical simulation to perform such things as grasp selection and trajectory planning. In addition, mobile robotics can use a mesh map to perform both path planning and obstacle avoidance. In general, a mesh is a useful representation to plan actions and simulate those actions since such simulation engines already exist from the gaming community.

The second area is teleoperation or Urban Search and Rescue (USAR). The work of Bruemmer et al. [72] and other similar works [73, 74] has shown that the most effective user interface is one which displays information in a similar way to many popular First-Person Shooter (FPS) video games such as Quake and Half-Life. The most natural way to build these types of interfaces is by rendering a mesh. Rendering techniques, hardware, and software have already been optimized for using meshes. Other types of representations can be displayed as a mesh, such as implicit functions. However, they require a post processing step. MABDI will build and maintain the mesh directly. The main impact of this work on USAR applications is that a much better mesh will be shown to the user than a mesh created through greedy methods, which is the current state of the art. The mesh presented will converge to the true environment over time. In addition, it will be able to operate in dynamic environments which have new or removed objects.

6 Approach

A clear idea of the algorithmic structure of MABDI is given by the System Flow Diagram in Figure 1. A basic description of the main variables can be found in Table 2. The inputs to the system are RGB-D data from a Kinect-style sensor D and the pose of the sensor P. The end goal of the system is to update the current mesh representation in each iteration. This update is represented by the

last step in the System Flow Diagram. We can see that the update step is primed by two distinct processes. In the diagram, each process is signified by a blue background. On the left hand side we have a process which is named the Triangulation Process. This process defines a triangulation T based on the current depth image. On the right hand side we have a process that is named the Categorization Process. This process categorizes the measurements based on the effect they will have on the model. This triangulation and categorization will be used by the update procedure to efficiently evolve the map based on the current sensor measurements.

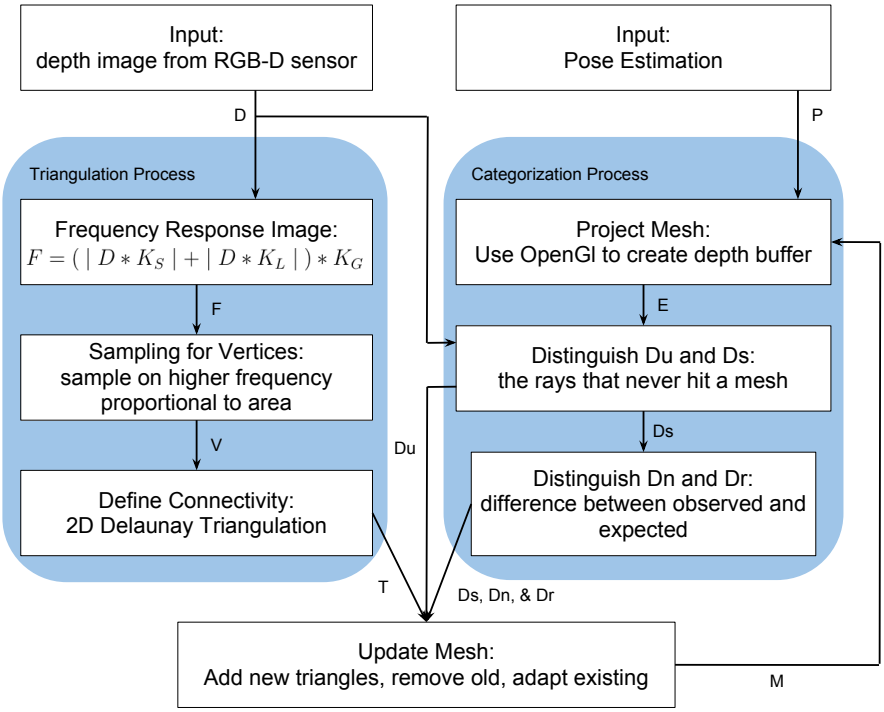

Figure 1: System Flow Diagram of MABDI

In the remaining sections of the Approach we will discuss the two processes which prime the update step in detail. Finally, we will discuss how the outputs are used to update the existing mesh map.

6.1 Triangulation Process

The goal of this process is to use the current depth image D to estimate a mesh of the current view of the environment. We can see a simplified system flow chart of this process in Figure 2. Also, we

Table 2: Basic description of the main variables

Variable Name	Description
D	Depth image from RGB-D sensor
F	Frequency response image
$K_S, K_L,$ and K_G	Image convolution operators
V and C	Mesh vertices and connectivity of the current triangulation
T	Current triangulation. Contains both V and C
P	The known pose of the sensor
E	Expected depth image
D_u	Previously *unseen* parts of D
D_s	Parts of D which *support* an existing part of M
D_n	Parts of D which correspond to a *new* object
D_r	Parts of D which correspond to a *removed* object
M	Current mesh

can see an example of the outputs of the process using an example input in Figure 3. It is important to remember that not all of these new elements will be used in the update. The decision of which elements from T to use will be based on the output of the Classification Process.

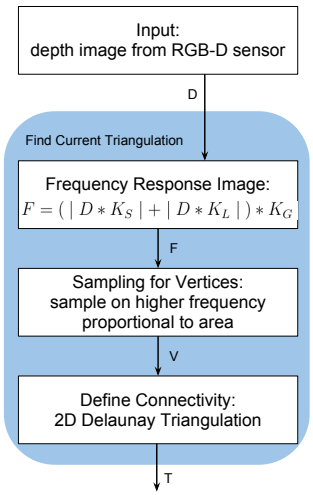

Figure 2: Flow Diagram of Current Triangulation Process

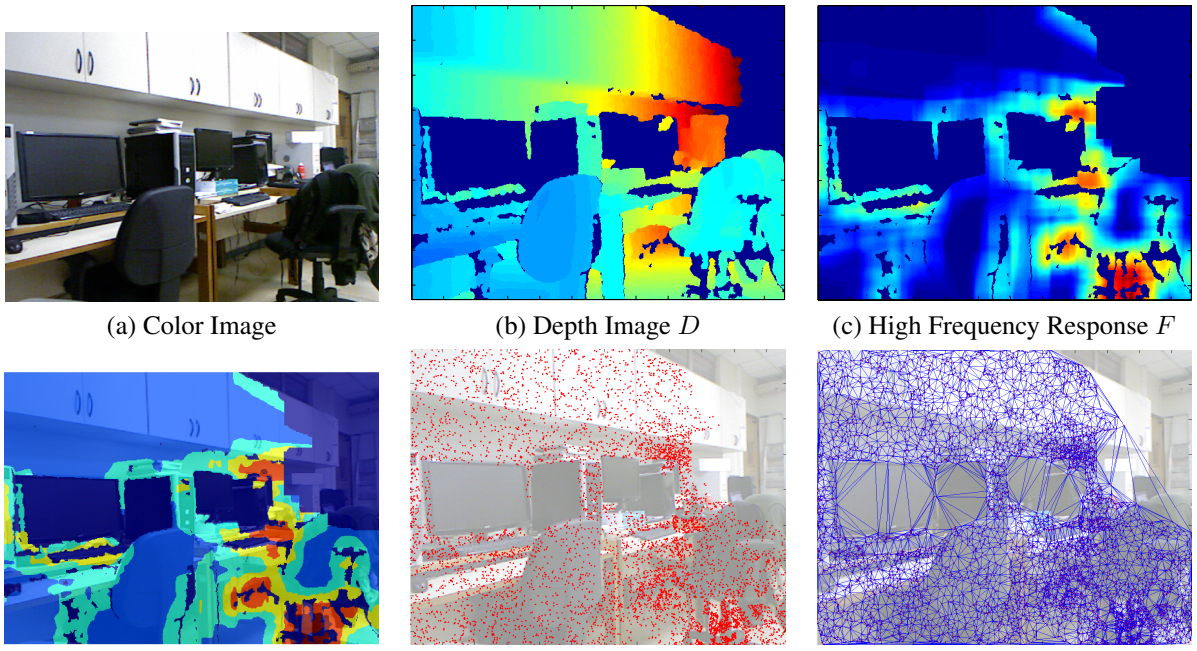

(a) Color Image (b) Depth Image D (c) High Frequency Response F

(d) After Histogramming F (e) Sampled Vertices V (f) Triangulation T

Figure 3: An example of the Triangulation Process. The idea is to start with a input depth image D and output a triangulation T which has a topology which is adaptive to the frequency content of the scene.

6.1.1 Frequency Response Image

The objective of this step is to use image processing techniques to quickly give an estimate of the frequency content in the depth image D. The end product will be an image F which is the same size as D and will have high values in regions with high change. In order to accomplish this we will use a sequence of image convolutions. Equation 1 gives the mechanics of the calculation. The Sobel operator K_S is used to give a response at corners since it is a first order differential operator. The Laplace operator K_L is used to generate a response in areas of curvature since it is a second order differential operator. The Gaussian operator K_G is used to spread the response to the neighboring areas.

$$F = (\mid D * K_S \mid + \mid D * K_L \mid) * K_G \tag{1}$$

K_S – small Sobel operator

K_L – small Laplace operator

K_G – large Gaussian operator

6.1.2 Histogram and Sample for Vertices

The objective of this section is to use the frequency response image F to create a set of vertices V. These vertices will be defined as locations in D. The idea is to have more vertices in regions of D that have a high frequency content. In order to accomplish this, we first define regions of similar frequency content by histogramming F. An example of this histogramming can be seen in Figure 3d. Next we will probabilistically sample F to define a set of vertices V. The probability of each pixel being sampled is given by Equation 2. The probability is calculated by the product of two different weights: W_F is based on the region of F where the measurement comes from and W_A is the proportional area of that region. The result of sampling for vertices can be seen in Figure 3e. In addition, because the probability of picking each pixel as a vertex can be calculated independently, the process is parallelizable.

$$p(u, v) = W_F(u, v) * W_A(u, v) \tag{2}$$

6.1.3 Determine Connectivity

Here we will use 2D Delaunay triangulation to define a connectivity between the set of vertices V found in the previous step. We are able to define the connectivity in $\mathbb{R}^2$ space because the topology is conserved as we project the elements into $\mathbb{R}^3$.

6.2 Classification Process

The goal of the classification process is to use the difference between the actual D and the expected depth image E to classify regions of the depth image D by the effect they will have on the model. The system flow diagram of the classification process can be seen in Figure 4. In order to generate an expected depth image E we will use the existing mesh map M and the known pose of the sensor P to create an artificial depth map of the what we expect the sensor to see E. We can then use image differencing and binary blob detection to segment regions of the depth map D.

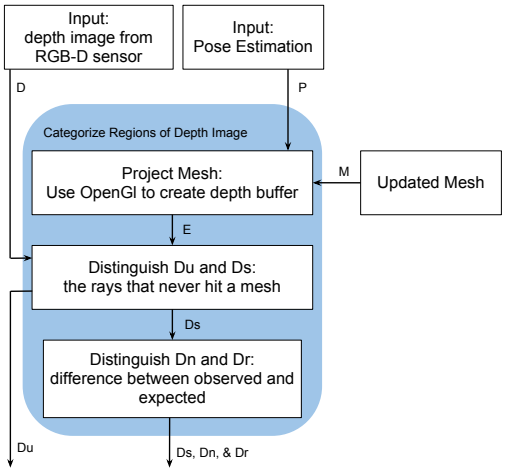

Figure 4: Flow Diagram of Categorize Measurements Process

6.2.1 Generate Expected Depth Image E

We will use an existing graphics code library named OpenGL to generate an expected depth image E. A similar approach was used by Fallon et al. in [75]. Figure 5 is a figure from Fallon's paper which gives a clear idea of the proposed method. The procedure will be to give the existing mesh model M and the current pose P to OpenGL and render a depth buffer. It is possible to define the intrinsic parameters of the sensor to match the actual sensor. Figure 5a and 5b give an example of this process. Figure 5b represents the output of this step being the expected depth image E. In addition, Figure 5d gives an example of D and also in Figure 5d we can see a RGB image of the scene.

6.2.2 Find Unknown Parts of the Scene

The objective of this step is to determine regions of the depth image D which correspond to areas of the environment that have never been seen before. This will be accomplished by finding regions of E that have no measurement. This occurs when the ray traced through the pixel never hits a mesh element. Regions which are unseen will be designated as D_u and the rest will be designated as D_s.

6.2.3 Find New and Removed Objects

The objective of this step is determine if measurements from the known region of the environment D_s correspond to new D_n or removed D_r objects in the scene. If they do not belong to D_n or D_r

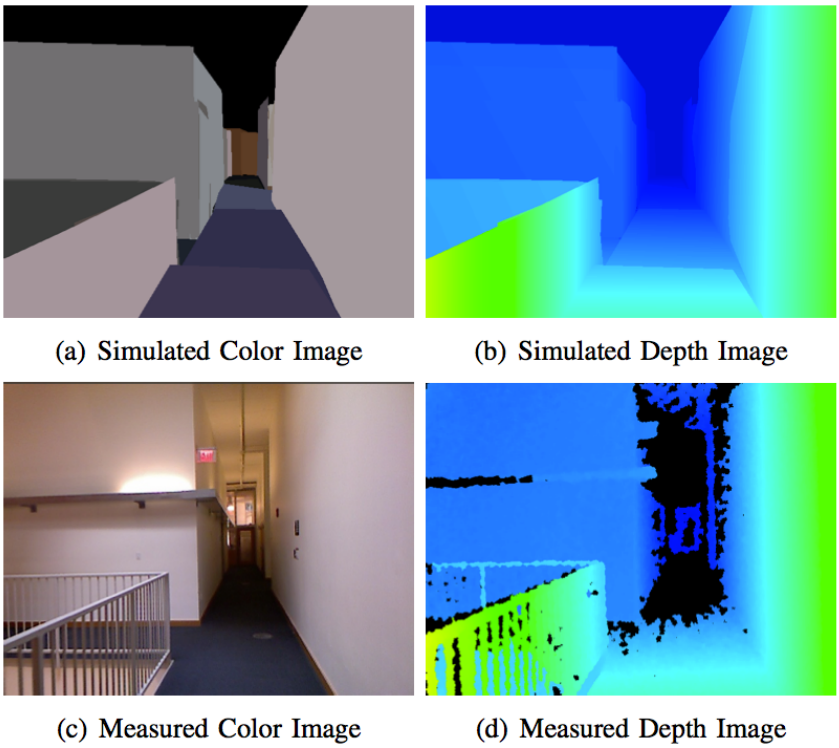

(a) Simulated Color Image (b) Simulated Depth Image

(c) Measured Color Image (d) Measured Depth Image

Figure 5: Work from [75] which generates an expected depth image E in the same way as the proposed method.

then they support an existing surface in the mesh map. Essentially they belong to a supporting region D_s until proven otherwise. In order to prove otherwise we will use image differencing between the expected E and the seen parts of the environment D_s. We will threshold the differenced image with $-\epsilon$ and $+\epsilon$ to make two distinct binary images. Blob analysis will then be run on this image to determine D_n and D_r.

6.3 Update Mesh

This is the last and most important step of MABDI. Here we will combine the triangulation T found in the Triangulation Process and the regions D_u, D_s, D_r, and D_n found from the Classification Process to efficiently update the existing mesh map M.

6.3.1 Add or Remove Mesh Elements

If the measurements in D correspond to new objects D_s or to unseen parts of the environment D_n, new mesh elements will need to be added. The new elements will come from the triangulation defined in T. In order to successfully merge the new elements with the existing mesh M the bordering vertices of the region will need to be found and stitched. It is proposed that this merging operation can be done in D.

If the measurements in D correspond to removed objects D_r, then the elements are removed from M. This is done by marking the vertices within the D_r region and deleting them and their connections.

6.3.2 Adapt Existing Mesh

Regions of the depth map which support an existing surface of the mesh model will be used to adapt the mesh in order to better approximate the real world. The idea of this process can be seen in Figure 6. In this figure the real world is represented by the blue surface in Figure 6a. The red dots represent the measurements from D. The mesh M is represented by the green surface. In the figure we see a single vertex being adjusted. In Figure 6b a set of planes are defined at the surrounding vertices and another plane is defined through the measurements which correspond to this particular vertex. This neighborhood of measurements will be found by defining a neighborhood in D. In Figure 6c the vertex is adjusted. This adjustment will be done by applying the Quadratic Error Measurement (QEM). The QEM will adjust the vertex to minimize the distance between all planes which were found in Figure 6b.

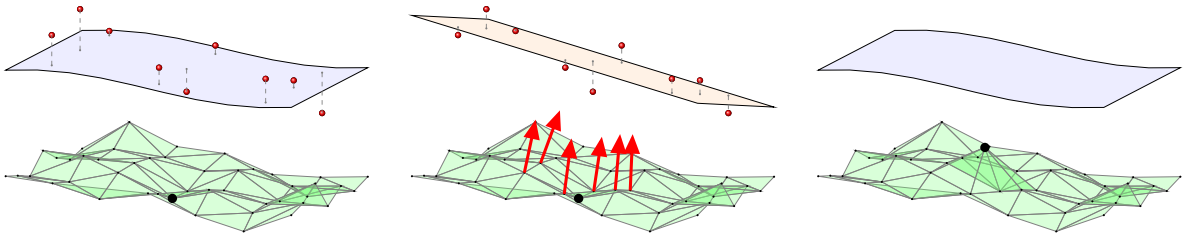

(a) Vertex with neighboring measurements

(b) Fitting a plane at neighboring vertices and through neighborhood of measurements

(c) Movement of vertex based on QEM

Figure 6: This shows the process of adapting a single vertex with new measurements.

7 Validation

In order to evaluate and quantify the effectiveness of MABDI, a series of experiments will be run in simulation. The reason for validating through simulation is that we will have control of all aspects of the experiment. In addition, we will have a known position of the sensor in a known environment. This will allow us to quantitatively measure our error. Figure 7 gives an idea of how the simulation will be accomplished. We will use a 3D modeling software named blender to create the environment and save it to a .ply file. Then, we will use OpenGl to open the .ply file and simulate readings from an RGB-D sensor. Finally, we will port these measurements to Matlab where MABDI will be developed and tested.

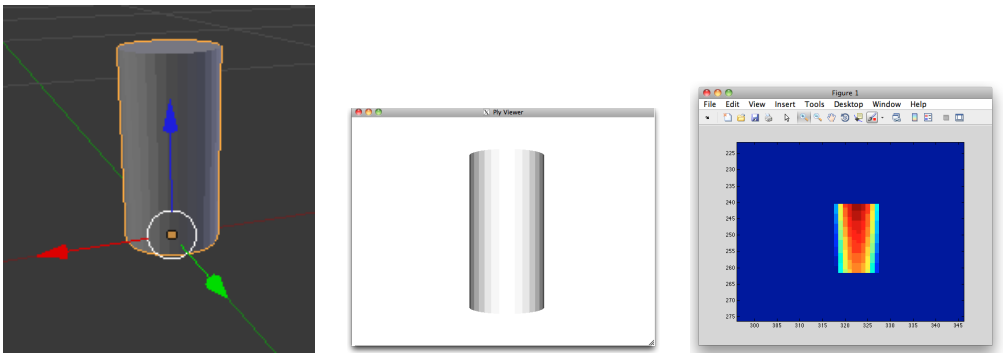

(a) Define geometry in Blender

(b) Render depth map in OpenGl

(c) Export depth image to Matlab

Figure 7: The steps of the simulation pipeline. The pipeline will allow us to simulate a RGB-D sensor viewing a known environment with a known pose.

With this simulation pipeline we can design a set of experiments that will sequentially test the abilities of MABDI. The idea will be to start with the easiest tests first in order make sure the system can map the environment under the most ideal conditions. Then, each subsequent experiment will aim to test a particular part of the system. By testing in this sequential manner we will be able to isolate and troubleshoot problematic parts of the system. Consequently, we will gain greater insight on the behavior of the system as a whole and the final system will be robust. The last experiment will test the robustness of the system with real world data. The following lists the proposed experiments and briefly describes the intention behind each experiment. For discussion purposes we can envision an environment which is made of a table and a can on the table.

1. Static scene; static object; static sensor
   Here we will test the system under the most ideal conditions. We want to see that the system

will categorize all measurements as D_S after the initial mesh is created. We will also test the ability of the system to adapt the current mesh over time.

2. Static scene; static object; dynamic sensor
   Here the sensor will move in the environment. For example, we can have it pan across the table by 1 meter. We want the system to recognize measurements which are from unseen parts of the environment and categorize them as D_U. Also, we want new elements to be added in unknown regions using the triangulation T from the Triangulation Process.

3. Dynamic scene; static object; static sensor
   This experiment will test the ability of the system to detect new and removed objects. We will do this by spontaneously adding and removing a second object in the scene such as another cup on top of the table. We will be looking for the system to successfully categorize the measurements as either D_N or D_R. We will then test the ability of the system to quickly remove or add the corresponding mesh elements from the current mesh.

4. Dynamic scene; dynamic object; static sensor
   This experiment will also test the ability of the system to react to new or removed object. However, the object will be moved into place over time. This will be a much more thorough testing of the Categorization Process and the ability to quickly add and remove elements.

5. Dynamic scene; dynamic object; dynamic sensor
   This experiment will test the entirety of the system in simulation. We can have the sensor circle the table while new elements are being added and removed.

6. Real world data
   This test will show the ability of the system to work with real world data from a RGB-D sensor. We will make use of an open source data set which is complete with pose information.

8 Tasks

There are six major phases which will need to be completed for this research. The following sections will list the steps which must be completed for each phase.

8.1 Simulation Pipeline

- Model all needed environments and object in Blender.
- Simulate a RGB-D sensor viewing the environments using OpenGL.

- Read in the simulated sensor output to Matlab.

8.2 Triangulation Process

- Calculate frequency response image F
- Sample F to obtain vertices V
- Triangulate vertices to obtain T

8.3 Classification Process

- Generate expected E from current mesh M
- Image differencing and blob analysis

8.4 Map Update

- Adaptation procedure
- Add/remove elements

8.5 Experiments

- Run validation experiments 1-6 as discussed in the Validation section.

9 Gantt Chart

In order to complete this work it will be necessary to plan the completion of the major tasks which were listed in the Tasks section. Figure 8 shows a Gantt Chart with the deadlines for each of the 5 major tasks and also shows the time needed for writing the Thesis. The Simulation Pipeline will be created first in order to have a database which will be used in code development of the other processes. It is important to note that some prior code development has been started and is represented by the gray portion of the task bars in Figure 8. I plan to defend my thesis by July 8th, 2013.

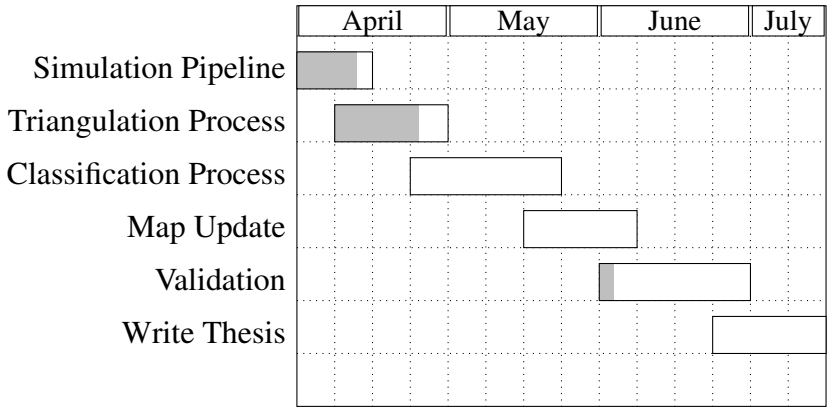

Figure 8: Gantt Chart

10 Committee

The committee members consist of:

- Dr. Ron Lumia - Department of Mechanical Engineering
- Dr. Rafael Fierro - Department of Electrical Engineering
- Dr. Robert Anderson - Sandia National Laboratories

References

[1] H. Durrant-Whyte and T. Bailey, "Simultaneous localization and mapping: part I," *Robotics & Automation Magazine*, 2006.

[2] T. Bailey and H. Durrant-Whyte, "Simultaneous localization and mapping (SLAM): Part II," *Robotics & Automation Magazine*, no. September, 2006.

[3] S. Thrun, "Robotic mapping: A survey," *Exploring artificial intelligence in the new millennium*, no. February, 2002.

[4] R. Smith, M. Self, and P. Cheeseman, "Estimating uncertain spatial relationships in robotics," *Autonomous robot vehicles*, 1990.

[5] S. Thrun, W. Burgard, and D. Fox, "A Probabilistic Approach to Concurrent Mapping and Localization for Mobile Robots," *Autonomous Robots*, vol. 25, pp. 1–25, 1998.

[6] J. Gutmann and K. Konolige, "Incremental mapping of large cyclic environments," in *Proceedings 1999 IEEE International Symposium on Computational Intelligence in Robotics and Automation. CIRA'99 (Cat. No.99EX375)*, pp. 318–325, IEEE, 1999.

[7] M. Dissanayake, P. Newman, S. Clark, H. Durrant-Whyte, and M. Csorba, "A solution to the simultaneous localization and map building (SLAM) problem," *IEEE Transactions on Robotics and Automation*, vol. 17, pp. 229–241, June 2001.

[8] S. Thrun, D. Fox, W. Burgard, and F. Dellaert, "Robust Monte Carlo localization for mobile robots," *Artificial Intelligence*, vol. 128, pp. 99–141, May 2001.

[9] M. Montemerlo, S. Thrun, D. Koller, and B. Wegbreit, "FastSLAM: A factored solution to the simultaneous localization and mapping problem," *Proceedings of the National conference on Artificial Intelligence*, pp. 593–598, 2002.

[10] S. Thrun, W. Burgard, and D. Fox, "A real-time algorithm for mobile robot mapping with applications to multi-robot and 3D mapping," in *Proceedings 2000 ICRA. Millennium Conference. IEEE International Conference on Robotics and Automation. Symposia Proceedings (Cat. No.00CH37065)*, vol. 1, pp. 321–328, IEEE, 2000.

[11] Y. Liu and R. Emery, "Using EM to learn 3D models of indoor environments with mobile robots," in *Machine Learning-International Workshop Then Conference*, 2001.

[12] A. Davison, "Real-time simultaneous localisation and mapping with a single camera," in *Proceedings Ninth IEEE International Conference on Computer Vision*, pp. 1403–1410 vol.2, IEEE, 2003.

[13] S. Thrun, D. Hahnel, D. Ferguson, M. Montemerlo, R. Triebel, W. Burgard, C. Baker, Z. Omohundro, S. Thayer, and W. Whittaker, "A system for volumetric robotic mapping of abandoned mines," in *2003 IEEE International Conference on Robotics and Automation (Cat. No.03CH37422)*, vol. 3, pp. 4270–4275, IEEE, 2003.

[14] A. Howard, D. Wolf, and G. Sukhatme, "Towards 3D mapping in large urban environments," *2004 IEEE/RSJ International Conference on Intelligent Robots and Systems (IROS) (IEEE Cat. No.04CH37566)*, vol. 1, pp. 419–424, 2004.

[15] D. Cole and P. Newman, "Using laser range data for 3D SLAM in outdoor environments," in *Proceedings 2006 IEEE International Conference on Robotics and Automation, 2006. ICRA 2006.*, pp. 1556–1563, IEEE, 2006.

[16] G. Klein and D. Murray, "Parallel Tracking and Mapping for Small AR Workspaces," in *2007 6th IEEE and ACM International Symposium on Mixed and Augmented Reality*, pp. 1–10, IEEE, Nov. 2007.

[17] L. Paz, P. Pinies, J. Tardos, and J. Neira, "Large-Scale 6-DOF SLAM With Stereo-in-Hand," *IEEE Transactions on Robotics*, vol. 24, pp. 946–957, Oct. 2008.

[18] K. Konolige and M. Agrawal, "FrameSLAM: From Bundle Adjustment to Real-Time Visual Mapping," *IEEE Transactions on Robotics*, vol. 24, pp. 1066–1077, Oct. 2008.

[19] H. Strasdat, J. Montiel, and A. Davison, "Scale drift-aware large scale monocular SLAM," *Proceedings of Robotics: Science and Systems (RSS). Vol. 2. No. 3. 2010*, 2010.

[20] N. Engelhard, F. Endres, and J. Hess, "Real-time 3D visual SLAM with a hand-held RGB-D camera," *Proc. of the RGB-D Workshop on 3D Perception in Robotics at the European Robotics Forum*, no. c, 2011.

[21] S. Rusinkiewicz and M. Levoy, "Efficient variants of the ICP algorithm," in *Proceedings Third International Conference on 3-D Digital Imaging and Modeling*, pp. 145–152, IEEE Comput. Soc, 2001.

[22] B. Yamauchi, A. Schultz, and W. Adams, "Mobile Robot Exploration and Map-Building with Continuous Localization," *Proceedings. 1998 IEEE International Conference on Robotics and Automation (Cat. No.98CH36146)*, vol. 4, no. May, pp. 3715–3720, 1998.

[23] A. Schultz and W. Adams, "Continuous localization using evidence grids," in *Proceedings. 1998 IEEE International Conference on Robotics and Automation (Cat. No.98CH36146)*, vol. 4, pp. 2833–2839, IEEE, 1998.

[24] R. Biswas, B. Limketkai, S. Sanner, and S. Thrun, "Towards object mapping in non-stationary environments with mobile robots," in *IEEE/RSJ International Conference on Intelligent Robots and System*, vol. 1, pp. 1014–1019, IEEE, 2002.

[25] A. Eliazar and R. Parr, "DP-SLAM 2.0," in *IEEE International Conference on Robotics and Automation, 2004. Proceedings. ICRA '04. 2004*, pp. 1314–1320 Vol.2, IEEE, 2004.

[26] M. Magnusson, A. Lilienthal, and T. Duckett, "Scan registration for autonomous mining vehicles using 3D-NDT," *Journal of Field Robotics*, vol. 24, pp. 803–827, Oct. 2007.

[27] A. Nüchter, K. Lingemann, J. Hertzberg, and H. Surmann, "6D SLAM3D mapping outdoor environments," *Journal of Field Robotics*, vol. 24, pp. 699–722, Aug. 2007.

[28] A. Huang, A. Bachrach, P. Henry, M. Krainin, D. Maturana, D. Fox, and R. Nicholas, "Visual odometry and mapping for autonomous flight using an RGB-D camera," pp. 1–16, 2011.

[29] F. Endres, J. Hess, N. Engelhard, J. Sturm, D. Cremers, and W. Burgard, "An evaluation of the RGB-D SLAM system," in *2012 IEEE International Conference on Robotics and Automation*, vol. 3, pp. 1691–1696, IEEE, IEEE, May 2012.

[30] R. A. Newcombe, A. J. Davison, S. Izadi, P. Kohli, O. Hilliges, J. Shotton, D. Molyneaux, S. Hodges, D. Kim, and A. Fitzgibbon, "KinectFusion: Real-time dense surface mapping and tracking," in *2011 10th IEEE International Symposium on Mixed and Augmented Reality*, pp. 127–136, IEEE, Oct. 2011.

[31] C. Martin and S. Thrun, "Real-time acquisition of compact volumetric 3D maps with mobile robots," in *Proceedings 2002 IEEE International Conference on Robotics and Automation (Cat. No.02CH37292)*, vol. 1, pp. 311–316, IEEE, 2002.

[32] D. Viejo and M. Cazorla, "Unconstrained 3D-Mesh Generation Applied to Map Building," *Progress in Pattern Recognition, Image Analysis and Applications*, vol. 3287, pp. 161–207, 2004.

[33] F. Giesen, "Delaunay Triangulation Based Surface Reconstruction: Ideas and Algorithms," no. November, 2004.

[34] J. Weingarten and R. Siegwart, "3D SLAM using planar segments," in *2006 IEEE/RSJ International Conference on Intelligent Robots and Systems*, pp. 3062–3067, IEEE, Oct. 2006.

[35] A. Akbarzadeh, J.-M. Frahm, P. Mordohai, B. Clipp, C. Engels, D. Gallup, P. Merrell, M. Phelps, S. Sinha, B. Talton, L. Wang, Q. Yang, H. Stewenius, R. Yang, G. Welch, H. Towles, D. Nister, and M. Pollefeys, "Towards Urban 3D Reconstruction from Video," in *Third International Symposium on 3D Data Processing, Visualization, and Transmission (3DPVT'06)*, pp. 1–8, IEEE, June 2006.

[36] M. Pollefeys, D. Nistér, J.-M. Frahm, A. Akbarzadeh, P. Mordohai, B. Clipp, C. Engels, D. Gallup, S.-J. Kim, P. Merrell, C. Salmi, S. Sinha, B. Talton, L. Wang, Q. Yang, H. Stewénius, R. Yang, G. Welch, and H. Towles, "Detailed Real-Time Urban 3D Reconstruction from Video," *International Journal of Computer Vision*, vol. 78, pp. 143–167, Oct. 2007.

[37] R. Pajarola, Y. Meng, and M. Sainz, "Fast Depth-Image Meshing and Warping," no. 02, 2002.

[38] J. Poppinga, N. Vaskevicius, A. Birk, and K. Pathak, "Fast plane detection and polygonalization in noisy 3D range images," in *Intelligent Robots and Systems (IROS) 2008*, pp. 3378–3383, Ieee, Sept. 2008.

[39] R. A. Newcombe and A. J. Davison, "Live dense reconstruction with a single moving camera," in *2010 IEEE Computer Society Conference on Computer Vision and Pattern Recognition*, pp. 1498–1505, IEEE, June 2010.

[40] Y. Ohtake, A. Belyaev, and H. Seidel, "A multi-scale approach to 3D scattered data interpolation with compactly supported basis functions," in *2003 Shape Modeling International.*, pp. 153–161, IEEE Comput. Soc, 2003.

[41] J. Stühmer, S. Gumhold, and D. Cremers, "Real-time dense geometry from a handheld camera," *Pattern Recognition*, pp. 11–20, 2010.

[42] P. Henry, M. Krainin, E. Herbst, X. Ren, and D. Fox, "RGB-D mapping: Using Kinect-style depth cameras for dense 3D modeling of indoor environments," *The International Journal of Robotics Research*, vol. 31, pp. 647–663, Feb. 2012.

[43] T. Weise, T. Wismer, B. Leibe, and L. Van Gool, "In-hand scanning with online loop closure," *2009 IEEE 12th International Conference on Computer Vision Workshops, ICCV Workshops*, pp. 1630–1637, Sept. 2009.

[44] H. Pfister, M. Zwicker, J. van Baar, and M. Gross, "Surfels : Surface Elements as Rendering Primitives," in *SIGGRAPH 2000*, (New York, New York, USA), pp. 335–342, ACM Press, July 2000.

[45] T. Whelan, M. Kaess, and M. Fallon, "Kintinuous: Spatially Extended KinectFusion," 2012.

[46] T. Whelan, H. Johannsson, M. Kaess, J. J. Leonard, and J. B. McDonald, "Robust Tracking for Real-Time Dense RGB-D Mapping with Kintinuous," Tech. Rep. MIT-CSAIL-TR-2012-031, Computer Science and Artificial Intelligence Laboratory, MIT, Sept. 2012.

[47] L.-K. Cahier, T. Ogata, and H. Okuno, "Incremental probabilistic geometry estimation for robot scene understanding," in *ICRA 2012*, pp. 3625–3630, Ieee, May 2012.

[48] M. Gopi and S. Krishnan, "A fast and efficient projection-based approach for surface reconstruction," in *SIBGRAPI02*, pp. 0–7, 2002.

[49] R. Mencl and H. Muller, "Interpolation and approximation of surfaces from three-dimensional scattered data points," *Scientific Visualization Conference, 1997*, 1997.

[50] W. E. Lorensen and H. E. Cline, "Marching cubes: A high resolution 3D surface construction algorithm," *Computer*, vol. 21, no. 4, pp. 163–169, 1987.

[51] H. Hoppe, T. DeRose, and T. Duchamp, *Surface reconstruction from unorganized points*. No. July 1992, 1992.

[52] H. Edelsbrunner and E. P. Mücke, "Three-dimensional alpha shapes," *ACM Transactions on Graphics*, vol. 13, pp. 43–72, Jan. 1994.

[53] J. Bloomenthal, "An Implicit Surface Polygonizer," *In Graphics Gems IV*, pp. 324–349, 1994.

[54] B. Curless and M. Levoy, "A volumetric method for building complex models from range images," in *SIGGRAPH '96*, pp. 303–312, 1996.

[55] K. Pulli, T. Duchamp, H. Hoppe, J. McDonald, L. Shapiro, and W. Stuetzle, "Robust meshes from multiple range maps," in *International Conference on Recent Advances in 3-D Digital Imaging and Modeling*, pp. 205–211, IEEE Comput. Soc. Press, 1997.

[56] H. Surmann, A. Nüchter, and J. Hertzberg, "An autonomous mobile robot with a 3D laser range finder for 3D exploration and digitalization of indoor environments," *Robotics and Autonomous Systems*, vol. 45, pp. 181–198, Dec. 2003.

[57] H. Zhao, S. Osher, and R. Fedkiw, "Fast surface reconstruction using the level set method," in *Variational and Level Set Methods in Computer Vision, 2001*, pp. 0–7, 2001.

[58] J. C. Carr, R. K. Beatson, J. B. Cherrie, T. J. Mitchell, W. R. Fright, B. C. McCallum, and T. R. Evans, "Reconstruction and representation of 3D objects with radial basis functions," *SIGGRAPH '01*, pp. 67–76, 2001.

[59] D. Terzopoulos and M. Vasilescu, "Sampling and Reconstruction with Adaptive Meshes," in *Computer Vision and Pattern Recognition, 1991. Proceedings CVPR '91.*, 1991.

[60] M. Vasilescu and D. Terzopoulos, "Adaptive meshes and shells: irregular triangulation, discontinuities, and hierarchical subdivision," in *Computer Vision and Pattern Recognition*, no. 1, pp. 3–6, IEEE Comput. Soc. Press, 1992.

[61] H. Hoppe, T. DeRose, T. Duchamp, J. McDonald, and W. Stuetzle, "Mesh Optimization," in *Proceedings of the 20th annual conference on Computer graphics and interactive techniques*, vol. d of *SIGGRAPH '93*, (New York, NY, USA), pp. 19–25, ACM, 1993.

[62] W.-C. Huang and D. Goldgof, "Adaptive-size meshes for rigid and nonrigid shape analysis and synthesis," *IEEE Transactions on Pattern Analysis and Machine Intelligence*, vol. 15, pp. 611–616, June 1993.

[63] M. Rutishauser, M. Stricker, and M. Trobina, "Merging range images of arbitrarily shaped objects," *Proceedings of IEEE Conference on Computer Vision and Pattern Recognition CVPR-94*, pp. 573–580, 1994.

[64] H. Delingette, "Simplex meshes: a general representation for 3D shape reconstruction," in *Computer Vision and Pattern Recognition*, pp. 856–859, 1994.

[65] G. Turk and M. Levoy, "Zippered polygon meshes from range images," in *SIGGRAPH '94*, (New York, New York, USA), pp. 311–318, ACM Press, 1994.

[66] Y. Chen and G. Medioni, "Description of Complex Objects from Multiple Range Images Using an Inflating Balloon Model," *Computer Vision and Image Understanding*, vol. 61, pp. 325–334, May 1995.

[67] F. Bernardini, J. Mittleman, H. Rushmeier, C. Silva, and G. Taubin, "The ball-pivoting algorithm for surface reconstruction," *IEEE Transactions on Visualization and Computer Graphics*, vol. 5, no. 4, pp. 349–359, 1999.

[68] M. Gopi, S. Krishnan, and C. Silva, "Surface reconstruction based on lower dimensional localized Delaunay triangulation," *Computer Graphics Forum*, vol. 19, no. 3, 2001.

[69] I. Ivrissimtzis, W.-K. Jeong, and H.-P. Seidel, "Using growing cell structures for surface reconstruction," *2003 Shape Modeling International.*, vol. 2003, pp. 78–86, 2003.

[70] M. Alexa, J. Behr, D. Cohen-Or, S. Fleishman, D. Levin, and C. Silva, "Point set surfaces," *Proceedings Visualization, 2001. VIS '01.*, pp. 21–537, 2004.

[71] Z. C. Marton, R. B. Rusu, and M. Beetz, "On fast surface reconstruction methods for large and noisy point clouds," in *2009 IEEE International Conference on Robotics and Automation*, pp. 3218–3223, IEEE, May 2009.

[72] D. Bruemmer, D. Few, R. Boring, J. Marble, M. Walton, and C. Nielsen, "Shared Understanding for Collaborative Control," *IEEE Transactions on Systems, Man, and Cybernetics - Part A: Systems and Humans*, vol. 35, pp. 494–504, July 2005.

[73] J. Drury, J. Scholtz, and H. Yanco, "Awareness in human-robot interactions," in *SMC'03 Conference Proceedings. 2003 IEEE International Conference on Systems, Man and Cybernetics. Conference*, vol. 1, pp. 912–918, IEEE, 2003.

[74] M. W. Kadous, R. K.-M. Sheh, and C. Sammut, "Effective user interface design for rescue robotics," in *Proceeding of the 1st ACM SIGCHI/SIGART conference on Human-robot interaction - HRI '06*, (New York, New York, USA), p. 250, ACM Press, Mar. 2006.

[75] M. F. Fallon, H. Johannsson, and J. J. Leonard, "Efficient scene simulation for robust monte carlo localization using an RGB-D camera," in *2012 IEEE International Conference on Robotics and Automation*, pp. 1663–1670, IEEE, May 2012.